

MASTER

Nonequilibrium Neutron Emission
from $^{12}\text{C} + ^{158}\text{Gd}$ and $^{13}\text{C} + ^{157}\text{Gd}$ Reactions*

F. Plasil, J. R. Beene, R. L. Ferguson, A. Gavron,^a
F. E. Obenshain, and G. R. Young
Oak Ridge National Laboratory, Oak Ridge, Tennessee 37830

G. A. Petitt
Georgia State University, Atlanta, Georgia 30303

K. Geoffroy Young,^b M. Jääskeläinen, and D. G. Sarantites
Washington University, St. Louis, Missouri 63130

C. F. Maguire
Vanderbilt University, Nashville, Tennessee 37235

Nonequilibrium particle emission associated with the ^{170}Yb composite system has been the subject of several recent investigations¹⁻⁵ at ORNL. These studies have included direct measurements of alpha particles³ and of neutrons^{2,5} associated with specific fusion and partial-fusion products, as well as deductions regarding nonequilibrium neutron emission (NNE) based on gamma-multiplicity data.^{1,4} NNE associated with evaporation residues (ER) was observed for the $^{12}\text{C} + ^{158}\text{Gd}$ system² at 152 MeV and for $^{16}\text{O} + ^{154}\text{Sm}$ (also at 152 MeV)⁵ but not for $^{20}\text{Ne} + ^{150}\text{Nd}$ at 175 MeV.² These observations indicated that projectile structure influences the probability of NNE. Studies of the energy dependence of NNE associated with ER were carried out by Sarantites et al.¹ for $^{12}\text{C} + ^{158}\text{Gd}$ and by Beene et al.⁴ for $^{16}\text{O} + ^{154}\text{Sm}$. Their conclusions were inferred from gamma-multiplicity data, but only after they had established a relationship between such results and direct neutron measurements.^{2,5} From these studies of the ^{170}Yb composite system, it was apparent that partial waves involved in the nonstatistical behavior were predominantly peripheral and that the generalized critical angular momentum model of incomplete fusion of Siwek-Wilczynska et al.,⁶ together with the "sum-rule" generalization of this model,⁷ can adequately account for many of the observed effects.³⁻⁵ One aspect of the results that was not understood in terms of the sum-rule model of Wilczynski et al.⁷ is the difference in NNE observed for the different projectiles. To remedy this apparent deficiency, Beene et al.⁴ have replaced the ground-state Q-values, Q_{gg} , that appear in expressions for the phase space factors⁷ with Q-values appropriate to the binary projectile fragmentation process. This modification

DISCLAIMER

This book was prepared as an account of work sponsored by an agency of the United States Government. Neither the United States Government nor any agency thereof, nor any of their employees, makes any warranty, express or implied, or assumes any legal liability or responsibility for the accuracy, completeness, or usefulness of any information, apparatus, product, or process disclosed, or represents that its use would not infringe privately owned rights. Reference herein to any specific commercial product, process, or service by trade name, trademark, manufacturer, or otherwise, does not necessarily constitute or imply its endorsement, recommendation, or favoring by the United States Government or any agency thereof. The views and opinions of authors expressed herein do not necessarily state or reflect those of the United States Government or any agency thereof.

EAB

DISCLAIMER

This report was prepared as an account of work sponsored by an agency of the United States Government. Neither the United States Government nor any agency Thereof, nor any of their employees, makes any warranty, express or implied, or assumes any legal liability or responsibility for the accuracy, completeness, or usefulness of any information, apparatus, product, or process disclosed, or represents that its use would not infringe privately owned rights. Reference herein to any specific commercial product, process, or service by trade name, trademark, manufacturer, or otherwise does not necessarily constitute or imply its endorsement, recommendation, or favoring by the United States Government or any agency thereof. The views and opinions of authors expressed herein do not necessarily state or reflect those of the United States Government or any agency thereof.

DISCLAIMER

Portions of this document may be illegible in electronic image products. Images are produced from the best available original document.

provided an explanation of the observed differences in NNE for the three projectiles, ^{12}C , ^{16}O , and ^{20}Ne .

The purpose of this work is to further consider the following two effects: (1) the energy dependence of NNE and (2) effects of projectile structure. Energy spectra and angular distributions of neutrons from reactions between ^{12}C and ^{158}Gd at bombarding energies of 150, 124, and 103 MeV and from reactions between ^{13}C and ^{157}Gd at 160, 140, and 110 MeV were measured. The experimental procedures are described in detail elsewhere.⁸ Typical neutron spectra are shown in Fig. 1 for the 150-MeV $^{12}\text{C} + ^{158}\text{Gd}$ and 160-MeV $^{13}\text{C} + ^{157}\text{Gd}$ cases. It is clear from the figure that there is no significant difference between the spectra obtained from the ^{12}C reactions and those from ^{13}C reactions. Thus we do not observe a projectile structure effect, in contrast to the earlier studies described above.

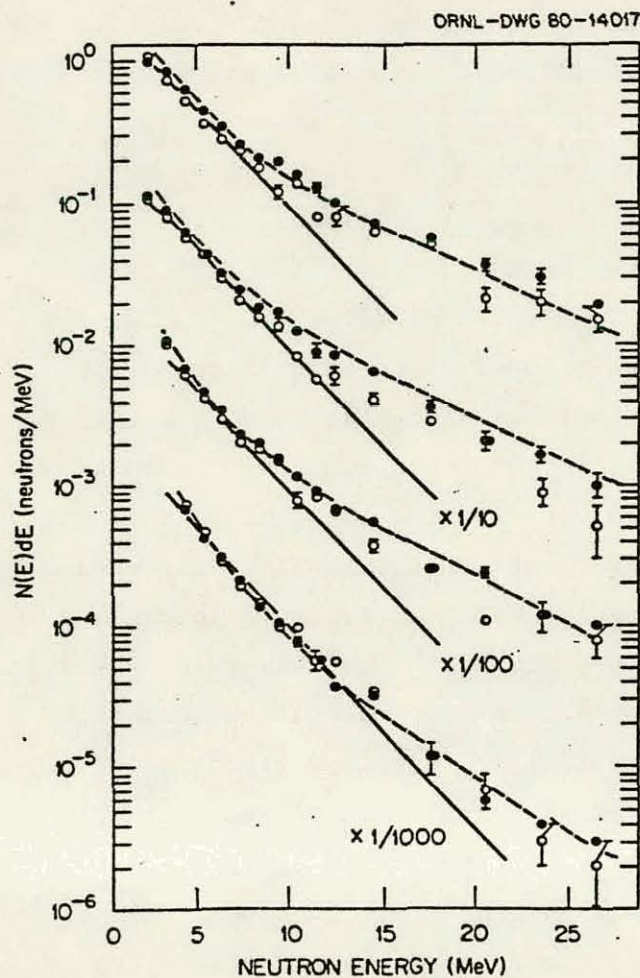


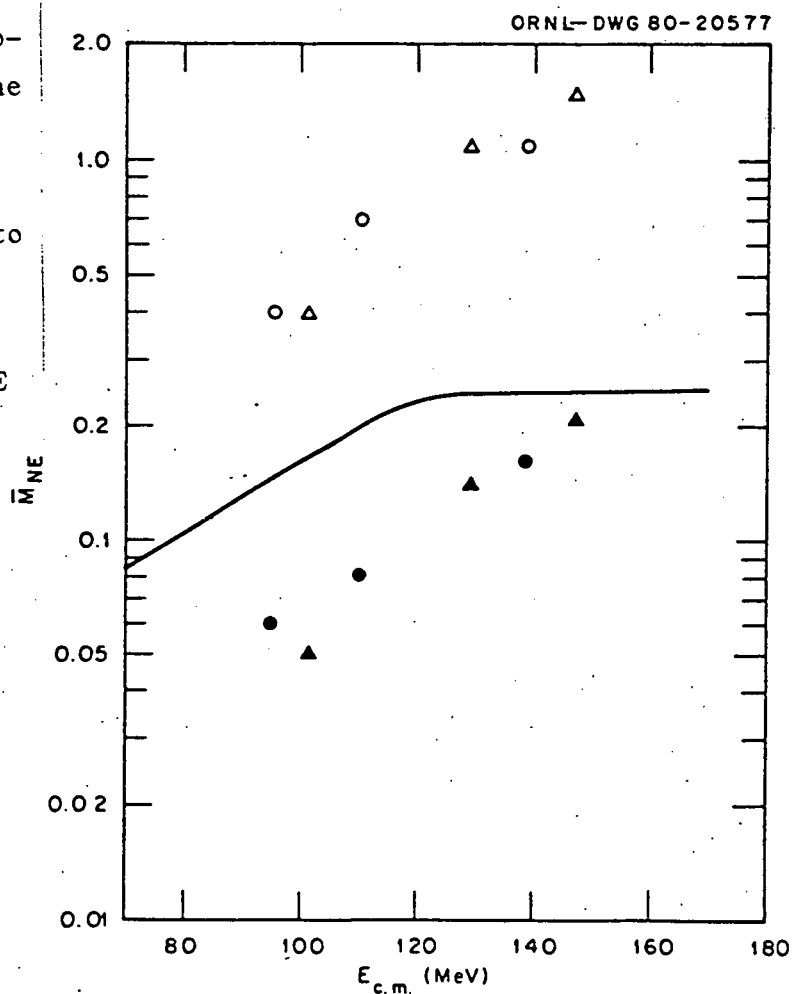
Fig. 1. Spectra of neutrons in coincidence with evaporation residues. Open circles: $^{12}\text{C} + ^{158}\text{Gd}$ (150 MeV); closed circles: $^{13}\text{C} + ^{157}\text{Gd}$ (160 MeV); average angles with respect to the beam (from top to bottom): 15.5, 32.5, 56.5, and 113.5 deg. The solid line is obtained by fitting the ^{12}C data using Eq. (1). The dashed line is obtained by fitting the ^{13}C data using the two-source model (see text).

In order to determine quantitatively the extent of NNE, it is necessary to subtract the contribution of evaporated neutrons from the measured spectra. Since there is no unique prescription to do this, we have used two methods which provide us with upper and lower limit estimates of NNE. The lower limit for NNE was obtained by ascribing all neutrons below 9 MeV to evaporation and by fitting the low-energy portion of the spectrum with

$$\phi(\epsilon) = \epsilon^{0.6} \exp[-\epsilon/T_{\text{Eq}}]. \quad (1)$$

The results of the fits are illustrated in Fig. 1. The NNE multiplicity for this case was obtained from the differences between the integrated experimental spectra and the integrals (at various angles) of Eq. (1). The results are shown in Fig. 2 for all systems studied.

Fig. 2. Average nonequilibrium neutron multiplicities. The curve was obtained from the Wilzcynski et al.⁷ sum-rule model. The open symbols refer to values from Table I and the closed symbols to values from the lower limit estimate of NNE (see text). Triangles are for $^{13}\text{C} + ^{157}\text{Gd}$ and circles for $^{12}\text{C} + ^{158}\text{Gd}$.



The upper limit for NNE was obtained by assuming that, in addition to the evaporation spectrum of Eq. (1), there exists another source of neutrons which has a higher temperature and which moves with a velocity V_{NE} greater than the velocity of the center of mass. We assumed the spectrum from this source to be given by

$$\phi_{NE}(\epsilon) = \epsilon \exp[-\epsilon/T_{NE}]. \quad (2)$$

A three-parameter fit was then performed to spectra at various angles. Equations (1) and (2) were used, and the variable parameters were T_{Eq} , T_{NE} , and V_{NE} . Results of the fits are given in Table I and illustrated in Fig. 1. The multiplicities obtained from integration of Eq. (2) are shown in Fig. 2.

The absence of differences in NNE between ^{12}C - and ^{13}C -induced reactions was surprising because of results of earlier studies^{2,5} and because a large effect was expected from the modified Fermi-jet calculations of Boneh et al.^{9,10} The sum-rule model of incomplete fusion of Wilczynski et al.⁷ was used to estimate the expected projectile structure effect. The result, expressed as the ratio of expected NNE cross sections for the two different projectiles, is shown in Fig. 3. Since the calculated value of the ratio is close to one at all bombarding energies, we conclude that agreement between experiment and theory is excellent in this respect. Also shown in Fig. 3 are curves obtained with the modifications of Ref. 7 by Beene et al.⁴ These modifications involved, as stated above, the replacement of Q_{gg} values with Q -values appropriate to projectile fragmentation. Two curves are shown in Fig. 3, based on the method of Ref. 4; they are calculated with different values of a level-density-related parameter. Both predictions are clearly at variance with our observations. We do not understand why the Wilczynski model explains our results (and those of Ref. 7), while modifications are required for an explanation of results of Refs. 2 and 4.

Other comparisons with the Wilczynski model have also been favorable. For example, the predicted NNE multiplicity is shown as a function of bombarding energy in Fig. 2. As expected, our results, which constitute upper and lower limits, bracket the calculated curve. The predicted leveling-off in the multiplicity at the highest bombarding energies has, however, not been observed.

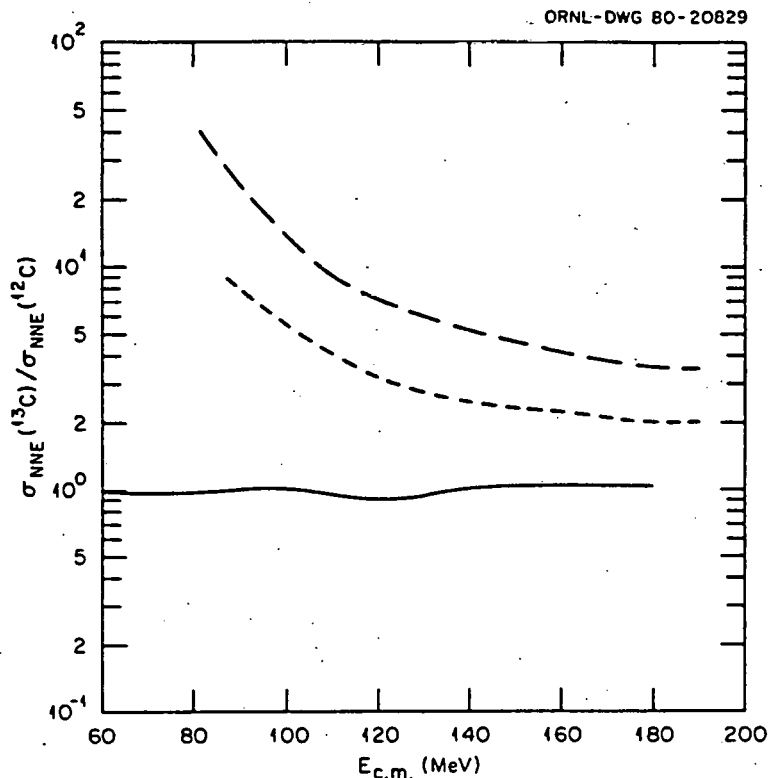


Fig. 3. Calculated ratio of NNE associated with ER for ^{13}C -induced reactions to NNE for ^{12}C -induced reactions. The solid curve is from the model of Wilczynski et al.⁷ The dashed curves are from a modified version of the model.⁴ Each of the two dashed curves refers to a different value of a level-density-related parameter.

From Fig. 1 it can be seen that our two-source parametrization is able to represent the data very well. While we must caution against taking such parametrizations literally, it is nevertheless interesting to speculate about the meaning of the two key parameters: the velocities and temperatures of the NNE sources. It can be noted from Table I that the velocity of the NNE source, V_{NE} , is intermediate between the velocity of the center of mass, $V_{\text{c.m.}}$, and the velocity of the projectile just prior to interaction, V_{B} , i.e., the velocity corresponding to the beam energy in excess of the Coulomb barrier. The ratio $V_{\text{NE}}/V_{\text{B}}$ ranges from 0.23 to 0.3. On the basis of a classical model⁴ we have estimated the tangential velocity of the projectile in the interaction region, V_{T} , from a Rutherford orbit. The orbital angular momentum was estimated from the incomplete-fusion model. The velocities V_{B} and V_{T} are shown in Fig. 4, together with the projection of V_{T} on the beam axis. It can be seen from

TABLE I. Parameters from the two-source description of NNE (see text).

Reaction	T_{Eq} (MeV)	T_{NE} (MeV)	$V_{\text{c.m.}}$ (cm/ns)	V_{B} (cm/ns)	V_{NE} (cm/ns)	\bar{M}_{Eq}	\bar{M}_{NE}
160-MeV ^{13}C	1.60	4.2	0.40	3.98	1.2	7.0	1.5
140-MeV ^{13}C	1.54	3.8	0.35	3.58	1.0	6.3	1.1
110-MeV ^{13}C	1.60	3.7	0.31	2.89	0.8	5.9	0.4
150-MeV ^{12}C	1.63	4.2	0.35	3.94	0.9	7.1	1.1
124-MeV ^{12}C	1.57	4.0	0.32	3.36	0.8	6.5	0.7
103-MeV ^{12}C	1.59	4.1	0.29	2.84	0.7	5.8	0.4
Error in parameter	± 0.03	± 0.1	-	-	± 0.1	± 0.2	± 0.1

T_{Eq} : temperature parameter in Eq. (1)

T_{NE} : temperature parameter in Eq. (2)

$V_{\text{c.m.}}$: c.m. velocity (provided for reference).

V_{B} : velocity of projectile in the interaction region (provided for reference)

V_{NE} : velocity of moving NNE source

\bar{M}_{Eq} : neutron evaporation multiplicity

\bar{M}_{NE} : NNE multiplicity

The assigned errors are the variation in the parameters that cause an increase of approximately 10% in chi-square.

the figure that the velocities of the NNE sources (Table I) are about a factor of two lower than the projection of V_T . The trend of V_{NE} with bombarding energy is, however, similar to that of V_T . From Table I it can be seen that the temperatures of the NNE sources are all approximately 4 MeV. Surprisingly, there does not appear to be any trend with increasing bombarding energy.

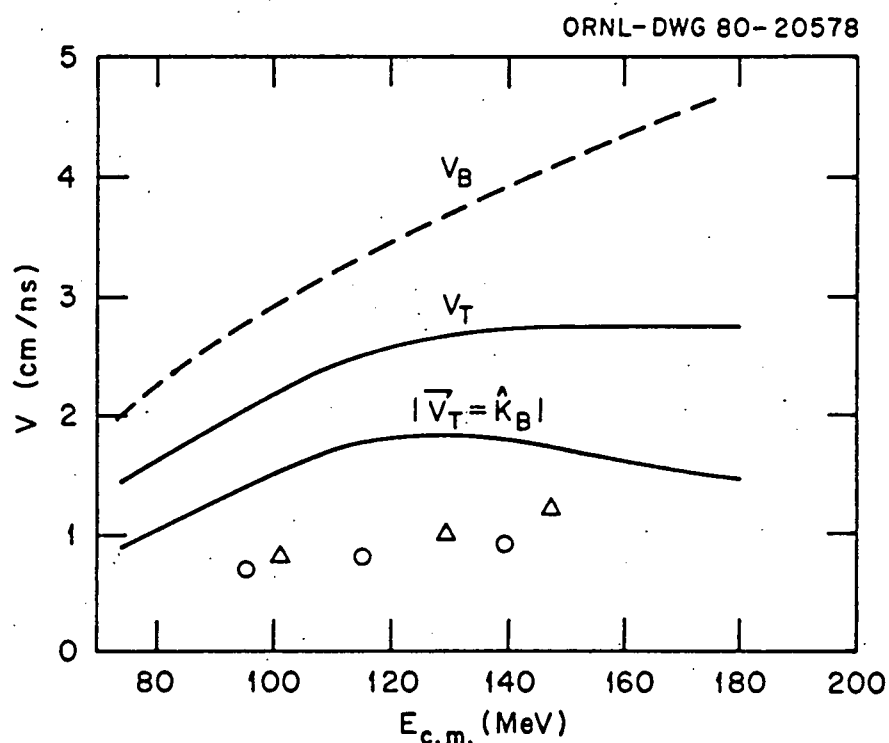


Fig. 4. Velocity as a function of c.m. bombarding energy. V_B (dashed curve) is the velocity of the projectile corresponding to its energy above the Coulomb barrier. V_T is the tangential velocity of the projectile at the time of interaction, and $|\vec{V}_T \cdot \hat{K}_B|$ is the projection of V_T on the beam direction. The data points are the velocities of the nonequilibrium source from Table I. Triangles refer to ^{13}C reactions and circles to ^{12}C reactions.

We have also investigated NNE associated with inelastic reactions for the systems discussed above. A detailed presentation will be made elsewhere.⁸ In this work we wish to point out only one particularly remarkable aspect of our results. It was noted that in cases in which a neutron detector was located at an angle close to the angle of the coincident heavy-ion telescope (in which the projectile-like fragment

was detected), a "bump" was observed in the neutron spectrum. From the neutron energy associated with the bump, it followed that the neutrons causing it had velocities similar to the projectile-like fragments. The bump was observed only for neutrons coincident with certain specific products (those with $Z = 5$ and 6 , primarily).

The observed structure is illustrated in Fig. 5 for the case of $124\text{-MeV } ^{12}\text{C} + ^{158}\text{Gd}$. Note that the bump appears only for coincident products with $Z = 5$ and 6 . A possible explanation of the observed structure is that it results from the decay of states in the projectile-like

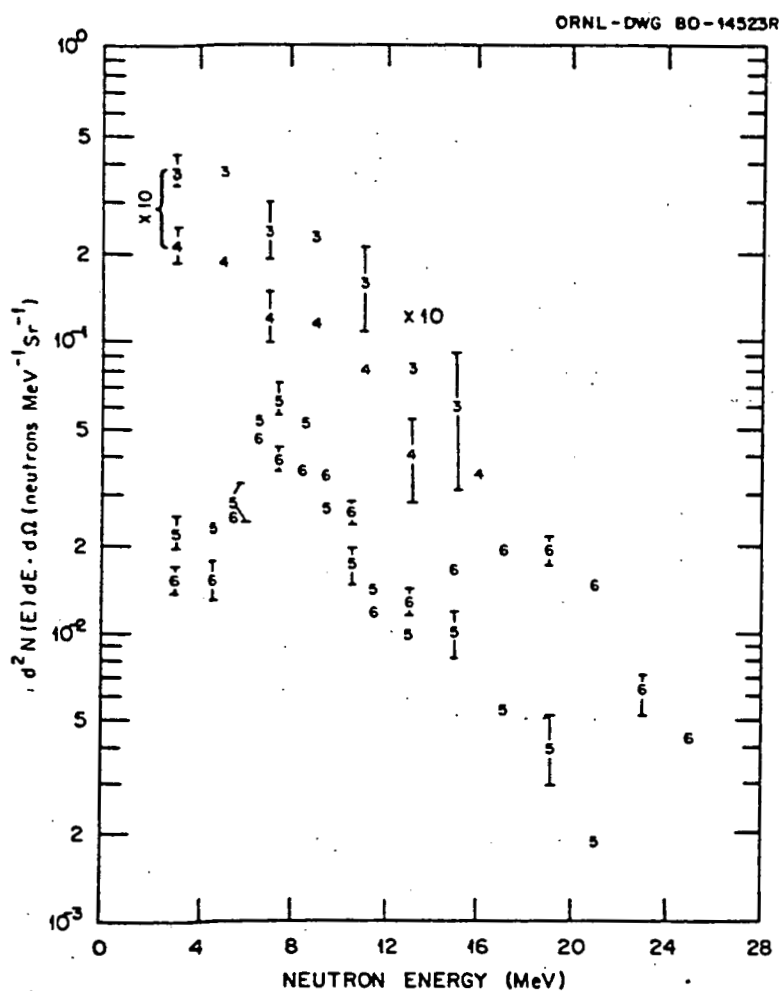


Fig. 5. Spectra of neutrons in coincidence with projectile-like fragments, having specific values of Z , from reactions between $124\text{-MeV } ^{12}\text{C} + ^{158}\text{Gd}$. The numbers of the data points indicate the nuclear charge of the projectile-like fragment with which the neutrons are in coincidence. Note the peaks in the neutron spectra associated with PLF's having $Z = 5$ and 6 .

fragment which have excitation energies that lie only slightly (≈ 100 keV) above the neutron separation energy for the particular nucleus involved. The decay of such states would result in neutron emission localized within a narrow cone about the direction of the projectile-like fragment. Due to the low kinetic energy released in the decay, the neutrons would have a narrow velocity distribution centered about the fragment velocity. It is possible to obtain estimates of the constraints on the level widths required by such a picture from estimates of the interaction times involved. From considerations based on rotation frequencies and on time required for Rutherford trajectories, we estimate the typical interaction time in our cases to be of the order of 5×10^{-21} s. If we require that the probability of decay of the excited state during this time be less than 10%, then the maximum permissible level width is about 15 keV.

We have examined known states with finite neutron widths, involving low kinetic energy release, for all nuclei with $Z = 3-6$ and $A = 6-15$. Only two levels, one in ^{12}B and the other in ^{14}C , satisfy the requirements. ^{12}B has a state at 3.3884 MeV (cf. $S_n = 3.369$ MeV) with $\Gamma_n < 1.4$ keV, and ^{14}C has a state at 8.3183 MeV (cf. $S_n = 8.1770$ MeV) with $\Gamma_n = 3.4 \pm 0.6$ keV. The fact that suitable states exist only in boron and carbon may explain why the bumps observed are predominantly associated with projectile-like fragments with $Z = 5$ and 6 .

References

*Research sponsored in part by the Division of High Energy and Nuclear Physics, U. S. Department of Energy, under contract W-7405-eng-26 with the Union Carbide Corporation.

^aPresent address: Los Alamos Scientific Laboratory, Los Alamos, New Mexico 87545.

^bPresent address: Fusion Energy Division, Oak Ridge National Laboratory, Oak Ridge, Tennessee 37830.

1. D. G. Sarantites, L. Westerberg, M. L. Halbert, R. A. Dayras, D. C. Hensley, and J. H. Barker, Phys. Rev. C 18, 774 (1978).
2. L. Westerberg, D. G. Sarantites, D. C. Hensley, R. A. Dayras, and J. H. Barker, Phys. Rev. C 18, 796 (1978).
3. K. A. Geoffroy, D. G. Sarantites, M. L. Halbert, D. C. Hensley, R. A. Dayras, and J. H. Barker, Phys. Rev. Lett. 43, 1303 (1979).
4. J. R. Beene, M. L. Halbert, D. C. Hensley, R. A. Dayras, K. Geoffroy Young, D. G. Sarantites, and J. H. Barker, to be published.
5. K. Geoffroy Young, D. G. Sarantites, J. R. Beene, M. L. Halbert, D. C. Hensley, R. A. Dayras, and J. H. Barker, to be published.
6. K. Siwek-Wilczynska, E. H. du Marchie van Voorthuysen, J. van Popta, R. H. Siemssen, and J. Wilczynski, Phys. Rev. Lett. 42, 1599 (1979); Nucl. Phys. A330, 150 (1979).

7. J. Wilczynski, K. Siwek-Wilczynska, J. van Driel, S. Gonggrijp, D.C.J.M. Hagemann, R.V.F. Jansens, J. Kukasiak, and R. H. Siemssen, Phys. Rev. Lett. 45, 606 (1980).
8. A. Gavron, J. R. Beene, R. L. Ferguson, F. E. Obenshain, F. Plasil, G. R. Young, G. A. Petitt, K. Geoffroy Young, M. Jaaskelainen, D. G. Sarantites, and C. F. Maguire, to be published.
9. Y. Boneh, A. Gavron, and S. Wald, Proceedings of the VII International Workshop on Gross Properties of Nuclei and Nuclear Excitations (Hirschegg, Austria, January 15-27, 1979).
10. Y. Boneh and A. Gavron, Proceedings of the International Symposium on Continuum Spectra of Heavy-Ion Reactions (San Antonio, Texas, December 3-5, 1979).